Coherent control of the dissociation probability of H_2^+ in ω-3ω two-color fields

Han Xu,[1] Hongtao Hu,[2] Xiao-Min Tong,[3] Peng Liu,[2,4,*] Ruxin Li,[2,4,†] Robert T. Sang,[1] and Igor V. Litvinyuk[1]

[1]*Centre for Quantum Dynamics, Griffith University, Nathan, Queensland 4111, Australia*

[2]*State Key Laboratory of High Field Laser Physics, Shanghai Institute of Optics and Fine Mechanics, Chinese Academy of Sciences, Shanghai 201800, China*

[3]*Center for Computational Sciences and Faculty of Pure and Applied Sciences, University of Tsukuba, Ibaraki 305-8577, Japan*

[4]*Collaborative Innovation Center of IFSA (CICIFSA), Shanghai Jiao Tong University, Shanghai 200240, China*

(Received 21 February 2016; published 17 June 2016)

We demonstrate that the coherent control of unimolecular reactions by using a waveform-controlled laser fields can lead to a strong modulation on the yield of the reaction. By using a synthesized ω (1800-nm) and 3ω (600-nm) two-color laser field, the probability of photodissociation of H_2^+ can be strongly modulated by varying the relative phase between the two colors. The dissociation probability maximizes at different relative phases for protons with different kinetic energy, and such energy dependence can also be qualitatively reproduced by our simulation. We attribute the observed dissociation probability modulation to the interference between two different dissociation pathways which start from the same electronic states and end with the same kinetic energy.

DOI: 10.1103/PhysRevA.93.063416

I. INTRODUCTION

To understand and control the process of laser-matter interaction is one of the ultimate goals of strong-field physics and physical chemistry. In particular, the dissociation of H_2^+ in an intense laser field, which is the simplest and most important prototype laser-induced molecular fragmentation process, has been extensively investigated experimentally and theoretically in the last few decades [1]. For example, ultrafast femtosecond laser pulses with controlled time evolution of the electric field has been used to steer the electron motion during the H_2^+ dissociation process, where the bound electron can be selectively localized to one of the two protons by waveform-controlled pulses (e.g., carrier-to-envelope-phase (CEP) controlled few-cycle pulses [2–5] and phase-controlled two-color femtosecond pulses) [6], as well as using attosecond EUV pump-femtosecond infrared probe pulses [7,8]. In addition to the control of the electron localization (or equivalently, the asymmetry of proton emission), Hua and Esry have predicted that the probability of the dissociation can also have a CEP dependence [9,10], where the CEP dependence is modulated with a shorter period of π than the asymmetry modulation period of 2π. Here the probability modulation means that the CEP of the driving laser field works as a "switch" for hydrogen dissociation, i.e., the dissociation channel can either be open (with enhanced probability) or closed (with suppressed probability) by controlling the CEP of the laser pulse. The predicted probability control has been examined in CEP-controlled experiments on a H_2 target [4] and a H_2^+ target [11,12], but the measured probability modulation turns out to be very weak (∼5% in Ref. [4], nonvisible in Ref. [11], and ∼11% in Ref. [12]), which is much weaker than the asymmetry modulation obtained in the same experiment (∼40% in Ref. [4], ∼10% in Ref. [11], and ∼30% in Ref. [12], correspondingly). And the probability modulation is the result of interference of $n-$ and $(n+2)$-photon absorption pathways, while the asymmetry modulation originates from the interference between $n-$ and $(n+1)$-photon absorption pathways [10]. Consequently, a much broader frequency bandwidth of the driving few-cycle pulses is required to obtain a probability modulation with similar amplitude as that of asymmetry modulation. As a result, the observed weak probability modulation can be partly explained by the limited spectral bandwidth of the few-cycle driving laser pulse. Ray *et al.* have investigated the coherent control over dissociative ionization of D_2 by using phase-controlled two-color (800-nm and 400-nm) pulses [6], where only a strong phase-dependent asymmetry modulation has been shown, while the phase-dependent dissociation probability controlling has not been addressed.

In order to improve the amplitude of dissociation probability modulation, which is too weak to be practical in the few-cycle pulse case, here we present a $\omega+3\omega$ two-color control scheme where the hydrogen molecule is dissociatively ionized by a two-color driving pulse which is synthesized from a mid-infrared fundamental pulse (1800 nm) and its third harmonic (600 nm). We show that the strong interference between a one-photon dissociation pathway (H_2^+ absorbs one 600 nm photon to dissociate) and a three-photon dissociation pathway (H_2^+ simultaneously absorbs three 1800-nm photons to dissociate) established in two-color fields can lead to a strong modulation (>50%) on the H_2^+ dissociation probability, which is approximately 1 order of magnitude higher than the previously reported modulation obtained in a few-cycle scheme.

The physical process of dissociative ionization of H_2 in the $\omega+3\omega$ two-color field can be described by the following simple picture. At the peak of the two-color pulses, the neutral H_2 molecule is singly ionized and transits from the ground state of neutral H_2 to the ground state ($1s\sigma_g$) of H_2^+, followed by the nuclear wave-packet motion due to the different equilibrium internuclear distances between H_2 and H_2^+. Once the internuclear separation of H_2^+ reaches a distance where the energy difference between ground state $1s\sigma_g$ and first dissociative state $2p\sigma_u$ equals the energy of a 600-nm photon, the H_2^+ can be excited to a dissociative $2p\sigma_u$ state via bond softening [13] (BS, one 600-nm absorption) or three-photon dissociation [14,15] (3PD, three 1800-nm photon absorption) pathways

*peng@siom.ac.cn
†ruxinli@mail.shcnc.ac.cn

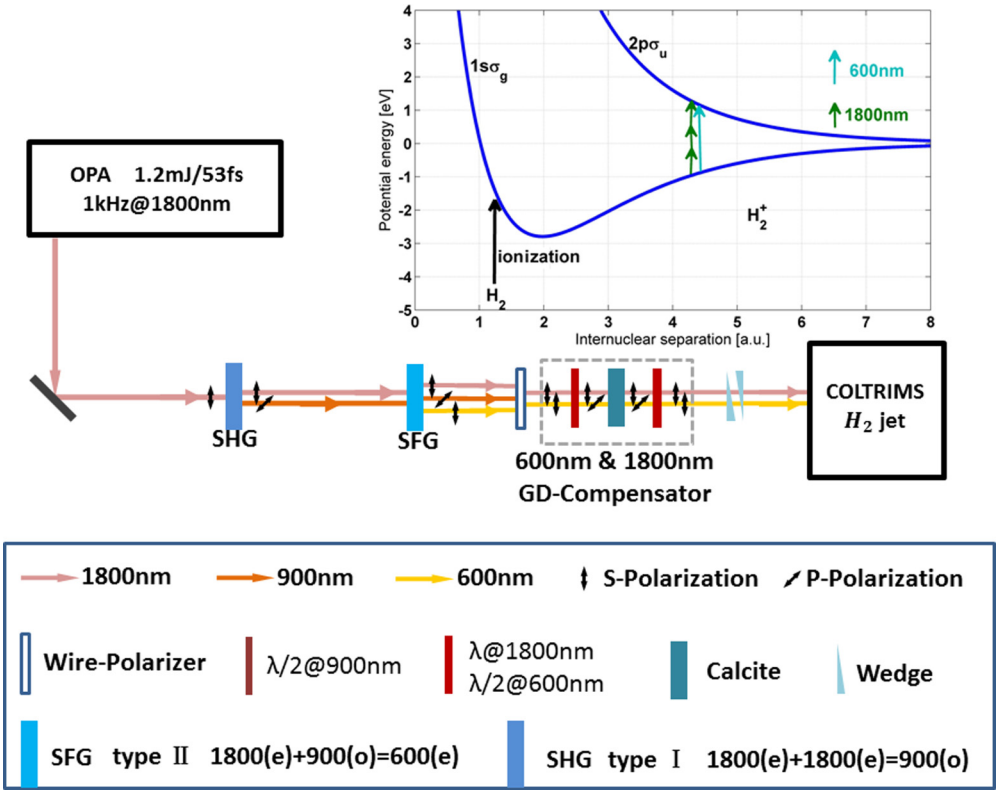

FIG. 1. Experimental setup includes an inline THG setup for generating synthesized 1800-nm and 600-nm two-color fields (see text for detailed descriptions) and COLTRIMS for measuring the momentum of protons. The two-color pulse is sent into COLTRIMS to dissociatively ionize a supersonic hydrogen molecule jet. Potential energy curves of the two lowest lying states of H_2^+, as well as the two possible dissociation pathways (three 1800-nm photon absorption and one 600-nm absorption), are shown in the upper-right subfigure.

resonantly. It is well known that control of electron localization is the result of the $\sigma_g - \sigma_u$ interference (i.e., interference between dissociation pathways along σ_g and σ_u states), where electronic states of σ_g and σ_u have opposite parity and the direction of electron localization is determined by the relative phase between the two states. As for the ω-3ω scheme, we are interested in $\sigma_u - \sigma_u$ interference (e.g., the interference between BS and 3PD dissociation pathways), which will result in an enhanced or suppressed dissociation probability by controlling the phase relationship of the two pathways.

II. EXPERIMENT

The schematic experimental setup is shown in Fig. 1. The ω-3ω two-color field is produced in an inline third harmonic generation (THG) setup. The linear-polarized midinfrared fundamental wave (FW, 1800 nm, 60 fs), delivered from a home-built 3-stage optical parametric amplifier (OPA) system [16] pumped by Ti:sapphire crystal (Coherent Elite) is frequency doubled in a type-I [$o(1800\,\text{nm}) + o(1800\,\text{nm}) \rightarrow e(900\,\text{nm})$] second-harmonic-generation (SHG) beta barium borate (BBO) crystal (thickness $= 200\,\mu$m, cut angle $= 20.2$ deg). Then a type-II [$e(1800\,\text{nm}) + o(900\,\text{nm}) \rightarrow e(600\,\text{nm})$] sum frequency generation (SFG) BBO crystal (thickness $= 400$, cut angle $= 25.7$ deg) is employed to generate the third harmonic pulse. The unnecessary SHG pulse, whose polarization axis is perpendicular to that of FW and THG, is filtered out by a wire grid polarizer. To compensate the group delay between parallel polarized FW and THG pulses, a GD compensator, which includes two polarization rotators (PR) (λ at 1800 nm and $\lambda/2$ at 600 nm) and a calcite crystal (thickness 790 μm, cut angle $= 90$ deg), is used. The first PR rotates the polarization axis of THG by 90 deg while keeping the axis of the FW pulse unchanged; then the group delay between the cross-polarized FW and THG pulses is compensated after passing through the calcite crystal. Finally the second PR rotates the polarization axis of THG back to be parallel to that of the FW pulse. The relative phase between the FW and THG pulse is controlled by a pair of fused silica wedges installed on a motorized linear stage. The output synthesized two-color field can be expressed as

$$E(t) = E_\omega \exp\left(-2\ln 2\frac{t^2}{\tau_\omega^2}\right)\cos(\omega t) + E_{3\omega}\exp\left(-2\ln 2\frac{(t+\Delta t)^2}{\tau_{3\omega}^2}\right)\cos(3\omega t + \Delta\phi), \quad (1)$$

with $E_\omega, E_{3\omega}$ being the field amplitude, τ_ω and $\tau_{3\omega}$ being the pulse duration (FWHM, around 60 fs in our experiment) of FW and THG pulses, respectively, and Δt being the group delay between the FW and THG pulses. The relative phase $\Delta\phi$ is controlled by changing the insertion of fused silica wedges from the position where $\Delta t \approx 0$. In the experiment, we scan the relative phase over a range of 6π with a

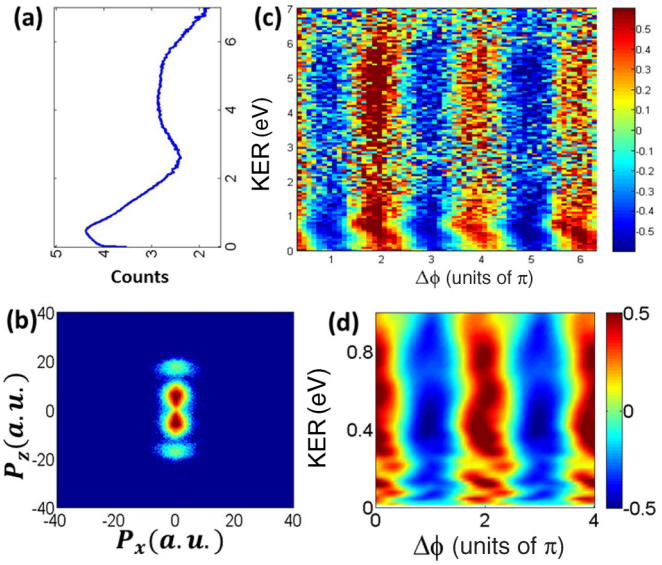

FIG. 2. Measured KER spectrum (a, in log scale) and momentum distribution in laser polarization plane (b, in logarithmic scale) for protons. (c) Measured P parameter for proton yield as a function of KER and relative phase. (d) The calculated P parameter for low-KER region, with similar FW and THG pulses as used in the experiment.

constant step size of $\pi/10$. We note that the group delay between the two pulses is only changed by ~4.6 fs during the phase scanning, which is negligible compared with their pulse duration of 60 fs. The resulting phase-controlled $\omega + 3\omega$ pulse is then launched into a COLTRIMS apparatus and focused by a concave mirror ($f = 75$ mm) onto a supersonic H_2 jet. The peak intensity of FW is calibrated by using the recoil momentum method [17] with a circular polarized pulse and found to be around 2×10^{14} W/cm^2. We estimate that the intensity of THG should not exceed 10% of the FW intensity. The full three-dimensional momentum of protons is measured by a time- and position-sensitive detector (RoentDek Handels GmbH). The polarization axis of both the FW and THG field are lying along the time-of-flight (TOF, z axis), which is perpendicular to the H_2 gas jet direction (y axis) and laser propagation direction (x axis).

III. RESULTS AND DISCUSSIONS

The measured phase-integrated proton kinetic-energy-release (KER) spectrum as well as momentum distribution in the laser polarization plane are shown in Figs. 2(a) and 2(b), correspondingly. The protons with low KER ($E < 2$ eV) come from H_2^+ dissociation pathways, while the protons with higher KER (3 eV $< E <$ 7 eV) mainly originate from an enhanced ionization (EI) channel [18–20], where the H_2^+ is further ionized at the critical internuclear distance and a pair of protons with higher KER is produced. The momentum distribution shows that the protons from both high- and low-KER regions are well confined to the small angles along the laser polarization axis, because the radiative coupling between σ_g and σ_u states as well as the enhanced ionization rate maximize with the molecular axis of H_2^+ parallel to the laser polarization. To characterize the depth of the probability modulation, we define parameter P as $P(E) = \frac{N(E)-\overline{N(E)}}{\overline{N(E)}}$, where $N(E)$ is the KER resolved total proton yield including both up yield ($N_{\rm up}$, with $p_z > 0$) and down yield ($N_{\rm down}$, with $p_z < 0$). $\overline{N(E)}$ is the yield averaged over all the phases. As most of the protons are emitted near the polarization axis, we only select those protons with the angle of emission within 30 deg for calculating the P parameter. The measured P as a function of KER and relative phase is shown in Fig. 2(c). Strong periodic phase-dependent modulation of the P parameter in the EI channel and dissociation channels is observed, which can be well fitted by the sine function $P = a\sin(\Delta\phi + c)$, where a is the modulation amplitude and c is the modulation phase. In the EI region with higher KER, the phase of the modulation shows no KER dependence, which gives rise to the straight vertical stripes in the spectrum shown in the upper half of Fig. 2(c). We attribute the P modulation in the EI channel to the variation of peak electric field strength of two-color fields for different $\Delta\phi$, where the EI yield should maximize with the laser peak electric field when $\Delta\phi$ is an integer number of 2π and so that the two-color fields can add constructively. This simple field strength dependence should be the same for protons with different KER, so the measured modulation in the EI region has no KER dependence. The EI yield modulation can be used for the calibration of the absolute value of $\Delta\phi$, where we set $\Delta\phi$, which corresponds to the maxima of EI yield as integer numbers of 2π. We note that the measured H_2^+ yield as a function of $\Delta\phi$ matches the EI yield modulation (not shown here). We also checked the asymmetry of electron localization in the $\omega + 3\omega$ two-color field and found no asymmetry for all $\Delta\phi$ scanned. This is simply due to the fact that the inversion symmetry of the $\omega + 3\omega$ synthesized laser field is not broken, which is different from the $\omega + 2\omega$ experiment [6].

It is interesting to note that the modulation phase shows a significant KER dependence in the lower KER region, and tilted stripes can be observed in the bottom half of Fig. 2(c). We compare the measured P modulation for KER around 0.3 eV and KER around 0.8 eV, as shown in Fig. 3(a), and the difference of the modulation phase is around 45 deg. The significant KER dependence on the modulation phase and modulation amplitude are clearly shown in Figs. 3(b) and 3(c). Such KER dependence cannot be explained by a simple field strength effect. In fact, the KER dependence has been predicted theoretically [10] and has been observed in many experiments addressing CEP-dependent asymmetry modulation [2–5] and yield modulation [4,11,12].

The KER-dependent modulation phase shift is also found in our simulation. We calculate the two-color field-induced dissociative ionization by solving the time-dependent Schrödinger equation which describes the time evolution of the nuclear wave packet (NWP) of H_2^+ :

$$i\frac{\partial}{\partial t}\begin{pmatrix}\psi_g(R,t)\\ \psi_u(R,t)\end{pmatrix} = \begin{pmatrix}-\frac{1}{2\mu}\frac{d^2}{dR^2} + E_g(R) & -D(R)E(t)\\ -D(R)E(t) & -\frac{1}{2\mu}\frac{d^2}{dR^2} + E_u(R)\end{pmatrix} \times \begin{pmatrix}\psi_g(R,t)\\ \psi_u(R,t)\end{pmatrix}, \quad (2)$$

where μ is the reduced mass of H_2, R the internuclear distance, $D(R)$ the transition dipole between the σ_g and σ_u states as a function of R, and $E(t)$ the time-dependent laser electric field.

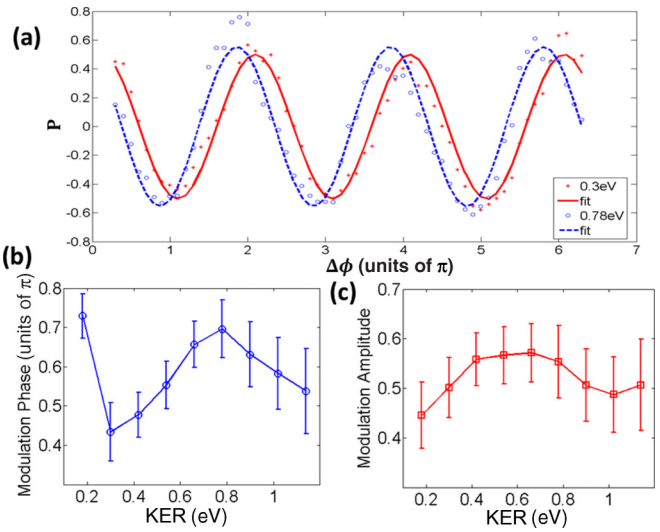

FIG. 3. (a) The measured P parameter as a function of $\Delta\phi$ for protons with KER of 0.3 eV (red star, with bin size of 0.04 eV) and KER of 0.78 eV (blue circle, bin size of 0.04 eV). Solid red line and blue dashed line are the corresponding sine fitting of the measured P modulation, where $p = a\sin(\Delta\phi + c)$ is used as the fitting function. (b), (c) KER-dependent modulation phase (c parameter) and amplitude (a parameter) with error bars, which is obtained in the sine fitting of the P parameter.

The potential energy curves and transition dipole strengths are calculated in prolate spheroidal coordinates as detailed in Ref. [21]. The peak intensity of FW is set as 2×10^{14} W/cm^2 and the intensity of the THG pulse as 2×10^{13} W/cm^2. The initial Frank-Condon NWP is assumed to be launched at each local maximum of the two-color laser field where the ionization rate of the neutral hydrogen molecule peaks and the NWP propagates in the rest of the laser field. The total dissociation yield is calculated by summing yields from each NWP incoherently, since the relative phases between those NWPs are unclear. Figure 2(d) shows the calculated $P(E)$ parameter for different relative phases. Similar to what we observed in the experiment, the probability modulation shows a strong KER dependence (i.e., tilting stripes) in the KER region of 0–1 eV. The details of the spectrum are different from the experimental measurement, which could possibly come from the assumptions we made for the initial NWP and the omission of the focal volume-averaging effects.

To get a better understanding of the dissociation probability modulation observed in our $\omega + 3\omega$ experiment, we follow the qualitative approach presented in Ref. [10], writing the kinetic-energy-dependent dissociation probability $D(E)$ as

$$D(E) = |e^{i\delta_u}e^{i\Delta\phi}\langle uE|F_1\rangle + e^{i\delta_u}\langle uE|F_3\rangle|^2, \qquad (3)$$

where only the interference of the BS dissociation pathway (one 3ω photon absorption, transition amplitude of $e^{i\delta_u}e^{i\Delta\phi}\langle uE|F_1\rangle$) and the TPD pathway (three ω photon absorption, transition amplitude of $e^{i\delta_u}\langle uE|F_3\rangle$) is taken into consideration, and all the other possible dissociation pathways are neglected to simplify the analysis. F_n ($n = 1,3$) is the Floquet representation of the nuclear wave function, E is KER of the dissociation process, and δ_u is the phase shift upon projection to σ_u ($|uE\rangle$). After expansion, Eq. (3) can be written as

$$D(E) = |\langle uE|F_1\rangle|^2 + |\langle uE|F_3\rangle|^2 + 2\mathrm{Re}(\langle uE|F_1\rangle\langle uE|F_3\rangle^*)\cos\Delta\phi, \qquad (4)$$

where the first two terms represent the constant background, the third term explains the observed 2π-periodic modulation as a function of $\Delta\phi$, and the observed KER dependence in the P spectrum [Figs. 2(c) and 2(d)] should come from the complex transition amplitudes $\langle uE|F_n\rangle$, which contain all the KER dependence. The measured modulation of dissociation probability is around 50%, as shown in Fig. 3(c). However, one cannot attribute the measured modulation completely to the interference effect, since the field strength effect can also modulate the rate of the first ionization ($H_2 \rightarrow H_2^+$), which in turn modulates the dissociation yield. So the modulation is a product of the interference-induced modulation and the field-strength-induced modulation. In spite of this, the interference effect should still dominate, because the measured KER dependence is significant while any field-strength-induced modulation should have no KER dependence.

IV. SUMMARY

To conclude, we show experimentally that the probability of dissociative ionization of H_2 in a $\omega + 3\omega$ two-color laser field can be controlled by varying the relative phase between FW and THG pulses, without modulating the asymmetry of the electron localization. In contrast to the previous experiments using a CEP-stabilized few-cycle pulse, a much stronger yield modulation (with period of 2π and amplitude $\sim$50%) can be achieved. It is interesting to note that the modulation shows significant KER dependence (45-deg shift of the modulation phase over a KER change of 0.5 eV in the low-KER region), and our numerical simulation qualitatively reproduced the observed KER dependence. The clear KER dependence of the probability modulation indicates that the dissociation probability control is mainly a result of quantum interference between different dissociation pathways rather than a simple field strength effect. The presented strong dissociation probability control by tailoring the driving pulse shape is a typical example of coherent control of molecular reaction. Our experiment shows that coherent control can not only alter the product ratios in a laser-induced reaction, which was originally proposed in [22], but also makes it possible to significantly increase the reaction yield along the desired pathway. The probability control, in combination with asymmetry control, will potentially improve overall control of molecular dynamics in a strong laser field.

ACKNOWLEDGMENTS

This work was supported by an Australian Research Council (ARC) Discovery Project (No. DP110101894), the ARC Centre for Coherent X-Ray Science (CE0561787), and by the National Science Foundation of China (11274326, 61221064, 11134010, and 11127901). H.X. was supported by an ARC Discovery Early Career Researcher Award (No. DE130101628). X.M.T. was supported by a Grand-in-Aid

for Scientific Research (C24540421) from the Japan Society for the Promotion of Science and a HA-PACS Project for advanced interdisciplinary computational sciences by exascale computing technology.

[1] M. F. Kling, P. von den Hoff, I. Znakovskaya, and R. de Vivie-Riedle, Phys. Chem. Chem. Phys. **15**, 9448 (2013).
[2] M. F. Kling, Ch. Siedschlag, A. J. Verhoef, J. I. Khan, M. Schultze, Th. Uphues, Y. Ni, M. Uiberacker, M. Drescher, F. Krausz *et al.*, Science **312**, 246 (2006).
[3] M. Kremer, B. Fischer, B. Feuerstein, V. L. B. Jesus, V. Sharma, C. Hofrichter, A. Rudenko, U. Thumm, C. D. Schröter, R. Moshammer *et al.*, Phys. Rev. Lett. **103**, 213003 (2009).
[4] H. Xu, J.-P. Maclean, D. E. Laban, W. C. Wallace, D. Kielpinski, R. T. Sang, and I. V. Litvinyuk, New J. Phys. **15**, 023034 (2013).
[5] H. Xu, T. Y. Xu, F. He, D. Kielpinski, R. T. Sang, and I. V. Litvinyuk, Phys. Rev. A **89**, 041403(R) (2014).
[6] D. Ray, F. He, S. De, W. Cao, H. Mashiko, P. Ranitovic, K. P. Singh, I. Znakovskaya, U. Thumm, G. G. Paulus *et al.*, Phys. Rev. Lett. **103**, 223201 (2009).
[7] G. Sansone, F. Kelkensberg, J. F. Pérez-Torres, F. Morales, M. F. Kling, W. Siu, O. Ghafur, P. Johnsson, M. Swoboda, E. Benedetti *et al.*, Nature (London) **465**, 763 (2010).
[8] K. P. Singh, F. He, P. Ranitovic, W. Cao, S. De, D. Ray, S. Chen, U. Thumm, A. Becker, M. M. Murnane *et al.*, Phys. Rev. Lett. **104**, 023001 (2010).
[9] F. Anis and B. D. Esry, Phys. Rev. A **77**, 033416 (2008).
[10] J. J. Hua and B. D. Esry, J. Phys. B: At. Mol. Opt. Phys. **42**, 085601 (2009).
[11] N. G. Kling, K. J. Betsch, M. Zohrabi, S. Zeng, F. Anis, U. Ablikim, Bethany Jochim, Z. Wang, M. Kübel, M. F. Kling *et al.*, Phys. Rev. Lett. **111**, 163004 (2013).
[12] T. Rathje, A. M. Sayler, S. Zeng, P. Wustelt, H. Figger, B. D. Esry, and G. G. Paulus, Phys. Rev. Lett. **111**, 093002 (2013).
[13] P. H. Bucksbaum, A. Zavriev, H. G. Muller, and D. W. Schumacher, Phys. Rev. Lett. **64**, 1883 (1990).
[14] S. Chelkowski, A. D. Bandrauk, A. Staudte, and P. B. Corkum, Phys. Rev. A **76**, 013405 (2007).
[15] I. V. Litvinyuk, A. S. Alnaser, D. Comtois, D. Ray, A. T. Hasan, J.-C. Kieffer, and D. M. Villeneuve, New J. Phys. **10**, 083011 (2008).
[16] C. Li, D. Wang, L. Song, J. Liu, P. Liu, C. Xu, Y. Leng, R. Li, and Z. Z. Xu, Opt. Express **19**, 6783 (2011).
[17] A. S. Alnaser, X. M. Tong, T. Osipov, S. Voss, C. M. Maharjan, B. Shan, Z. Chang, and C. L. Cocke, Phys. Rev. A **70**, 023413 (2004).
[18] T. Zuo and A. D. Bandrauk, Phys. Rev. A **52**, R2511(R) (1995).
[19] G. N. Gibson, M. Li, C. Guo, and J. Neira, Phys. Rev. Lett. **79**, 2022 (1997).
[20] Han Xu, Feng He, D. Kielpinski, R. T. Sang, and I. V. Litvinyuk, Sci. Rep. **5**, 13527 (2015).
[21] Ying-Jun Jin, Xiao-Min Tong, and Nobuyuki Toshima, Phys. Rev. A **86**, 053418 (2012).
[22] P. Brumer and M. Shapiro, Chem. Phys. Lett. **126**, 541 (1986).